Photoinduced Electron Transfer in Pentaammineruthenium(II) Complexes of 1-(4-Cyanophenyl)imidazole

Antonios Hatzidimitriou,[†] André Gourdon,[†] Jean Devillers,[†] Jean-Pierre Launay,*[,†] Elena Mena,[‡] and Edmond Amouyal*[,‡]

Molecular Electronics Group and Materials Chemistry and Modelization Group, Centre d'Elaboration de Matériaux et d'Etudes Structurales, CNRS, 29 rue Jeanne Marvig, 31 055 Toulouse Cedex, France, and Laboratoire de Physico-Chimie des Rayonnements, Bat. 350, Université Paris-Sud, 91 405 Orsay, France

Received April 21, 1995[⊗]

A new bridging ligand, 1-(4-cyanophenyl)imidazole (CPI) has been prepared, as well as its N-methylated derivative 1-methyl-3-(4-cyanophenyl)imidazolium iodide (CPI-Me^+I^-). The mononuclear and binuclear complexes $[(NH_3)_5Ru-CPI-Me]^{3+}$ and $[(NH_3)_5Ru\text{-}CPI\text{-}Ru(NH_3)_5]^{4+}$ have been obtained. Free CPI is planar, according to theoretical calculations (MMX and MNDO), and its luminescence properties suggest the occurence of a twisted internal charge transfer (TICT) state. The comparison of the two ruthenium complexes reveals the spectral and electrochemical features of coordination by the cyanophenyl or by the imidazole groups. Controlled oxidation of the binuclear complex $[(NH_3)_5Ru-CPI-Ru(NH_3)_5]^{4+}$ yields the mixed valence species $[(NH_3)_5Ru-CPI-Ru(NH_3)_5]^{5+}$ in which the ruthenium coordinated to the cyanophenyl group is ruthenium(II) while the ruthenium linked to imidazole is ruthenium(III). An intervalence band is observed at 640 nm ($\epsilon = 188$), from which the effective metal−metal coupling through the bridging ligand is determined as 0.032 eV. This value is satisfactorily reproduced by a theoretical calculation using the effective Hamiltonian theory. Finally the binuclear complex exhibits a weak luminescence when excited either on the ligand band near 260 nm or on the metal-to-ligand charge transfer band near 410 nm. The CPI ligand is the first example of a TICT-forming species with appreciable coupling between metallic sites and can be considered as a first step toward a molecular switch.

Introduction

The achievement of molecular switching is one of the main challenges of molecular electronics.[1] In the framework of a general study devoted to potential molecular switches, we have undertaken the study of pentaammineruthenium complexes with ligands exhibiting a special photophysical behaviour. An interesting possibility is to use the so called twisted internal charge transfer (TICT) effect.[2,3] It arises in certain donor−acceptor molecules which are planar in the ground state, the most typical being (dimethylamino)benzonitrile (DMABN).[3] Upon photochemical excitation, two excited states are successively generated: first a planar Franck Condon state, which is weakly polar, and then a twisted and strongly polar state. These two states are usually characterized by a dual luminescence with two clearly resolved emission bands in the visible region.[3] The large conformational change associated with twisting has strong consequences on orbital overlaps and thus on the electronic coupling between donor and acceptor, which makes this effect appealing for molecular switching.

In a previous study, we have described a bridging TICT molecule, namely bis (4-cyanophenyl) piperazine (BCPPZ).[4,5] The molecule consists of three parts, which are almost coplanar in the ground state: a central piperazine ring and two outer cyanophenyl groups. Time-resolved luminescence and transient absorption studies show that the TICT effect occurs, at least in the free ligand.[5] But the coupling efficiency of the molecule acting as bridging ligand for two metal sites is very small, even in the almost planar ground state, because of a lack of conjugation through the central piperazine ring.[6] In the present paper, we describe another system, 1-(4-cyanophenyl)imidazole, which presents analogous properties, but in addition a detectable coupling, measured by an intervalence transition in a binuclear complex.

Experimental Part and Computation Techniques

Diethyl ether was dried by distillation over sodium/benzophenone and methanol by distillation according to standard procedures. Other solvents were used without further purification. Air sensitive compounds (ruthenium complexes) were handled using standard Schlenk/cannula techniques.

1-(4-Cyanophenyl)imidazole (CPI). The reaction between 1.2 g (10 mmol) of 4-fluorobenzonitrile (Aldrich) and an excess (≈3.0 g) of imidazole (Aldrich) in 20 mL of DMSO was performed at 90 °C for 4 days. The solution was precipitated with 300 mL of water and the resulting white solid recrystallized several times, first in methanol and then in acetone. Yield with respect to fluorobenzonitrile: 86%.

* To whom correspondence should be addressed.
[†] CEMES, Toulouse.
[‡] Université Paris-Sud.
[⊗] Abstract published in *Advance ACS Abstracts,* March 1, 1996.

(1) Joachim, C.; Launay, J.-P. *J. Mol. Electron.* **1990**, *6*, 37. Gourdon, A. *New J. Chem.* **1992**, *16*, 953. Gilat, S. L.; Kawai, S. H.; Lehn, J.-M. *J. Chem. Soc., Chem. Commun.* **1993**, 1439.
(2) See for instance Rettig, W.; *Angew. Chem., Int. Ed. Engl.* **1986**, *25*, 971. Grabowski, Z. R.; Rotkiewicz, K.; Siemiarczuk, A.; Cowley, D. J.; Baumann, W. *Nouv. J. Chim.* **1979**, *3*, 443 and references therein.
(3) Lippert, E.; Rettig, W.; Bonacic-Koutecky, V.; Miehé, J. A., Heisel, F. *Adv. Chem. Phys.* **1987**, 68, 1. LaFemina, J. P., Duke, C. B.; Paton, A. *J. Chem. Phys.* **1987**, *87*, 2151. Su, S. G.; Simon, J. D. *J. Chem. Phys.* **1988**, *89*, 908. Kato, S.; Amatatsu, Y. *J. Chem. Phys.* **1990**, *92*, 7241. Majumdar, D.; Sen, R.; Bhattacharyya, K. Bhattacharyya, S. P. *J. Phys. Chem.* **1991**, *95*, 4324. Schenter, G. K.; Duke, C. B. *Chem. Phys. Lett.* **1991**, *176*, 563.
(4) Launay, J.-P.; Sowinska, M.; Leydier, L.; Gourdon, A.; Amouyal, E.; Boillot, M.-L.; Heisel, F.; Miehé, J. A. *Chem. Phys. Lett.* **1989**, *160*, 89.
(5) Gourdon, A.; Launay, J.-P.; Bujoli-Doeuff, M.; Heisel, F.; Miehé, J. A.; Amouyal, E.; Boillot, M.-L. *J. Photochem. Photobiol. A : Chem.* **1993**, *71*, 13.
(6) Launay, J.-P. In *Molecular Electronics-Science and Technology*; Aviram, A., Ed., Engineering Foundation: New York, 1989; p 237.

0020-1669/96/1335-2212$12.00/0

Table 1. Crystal Data for [CPI-Me](PF_6)·0.5CH_3COCH_3

chem formula	$[C_{11}H_{10}N_3][PF_6]\cdot 0.5C_3H_6O$
fw	329.18 + 29.04 (solvent)
cryst system	monoclinic
space group	$P2_1/c$
a (Å)	18.239(2)
b (Å)	12.0239(9)
c (Å)	15.235(2)
β (deg)	111.029(9)
V (Å^3)	3118.7(8)
Z	8
ρ_{calcd} (Mg m^{-3})	1.53
residual electron density max (e Å^{-3})	+0.36
residual electron density min (e Å^{-3})	−0.26
R	0.049
R_w	0.057

Anal. Calcd for $C_{10}H_7N_3$: C, 71.00; H, 4.14; N, 24.85. Found: C, 70.21; H, 4.38; N, 24.86.

IR (KBr, cm^{-1}): 3409 vs br, 3129 s, 2227 vs, 1610 vs, 1523 vs, 1488 s, 1426 w, 1306 s, 1265 s, 1185 w, 1101 w, 1059 vs, 961 w, 904 w, 836 vs, 732 s, 655 s, 551 s.

^{1}H NMR (CD_3OD, 250 MHz): 7.24 (s, 1H, *e*), 7.74 (s, 1H, *d*), 7.84 (d, 2H, 7Hz, *b*), 7.95 (d, 2H, 7Hz, *c*), 8.35 (s, 1H, *a*) (see Figure 1 for proton nomenclature).

UV−vis in methanol: 266 nm (ϵ = 21 220).

1-Methyl-3-(4-cyanophenyl)imidazolium Iodide (CPI-Me$^+$I$^-$) and Hexafluorophosphate (CPI-Me$^+$PF$_6^-$). Reaction of 1.69 g (10 mmol) of CPI and excess (≈5 mL) iodomethane (Aldrich) in 30 mL of dichloromethane was performed at 45 °C for 4 h. The final white-yellow precipitate was filtrated and dried under vacuum. It was recrystallized several times first from acetone and then from water. Yield with respect to CPI: 89%.

Anal. Calcd for $C_{11}H_{10}N_3I$: C, 42.44; H, 3.21; N, 13.50. Found: C, 42.20; H, 3.38; N, 13.70.

IR (KBr, cm^{-1}): 3443 vs, 3096 s, 2925 s, 2233 s, 1600 s, 1573 s, 1547 vs, 1510 w, 1348 w, 1308 w, 1237 s, 1067 w, 847 vs, 615 w, 552 s.

^{1}H NMR (CD_3OD, 250 MHz): 4.11 (s, 3H, *f*), 7.88 (d, 2H, 9Hz, *e*), 7.98 (d, 2H, 9Hz, *b*), 8.09 (d, 2H, 9Hz, *c*), 8.22 (d, 1H, 2Hz, *d*), 9.68 (s, 1H, *a*) (see Figure 1 for proton nomenclature).

UV−vis in methanol: 254 nm (ϵ = 10 200).

The hexafluorophosphate was prepared by dissolving the iodide in water, and precipitating by sodium hexafluorophosphate. Redissolution in aceton and addition of an equivalent volume of ether yielded crystals as colorless plates after 3 or 4 days at 4 °C.

Anal. Calcd for dried $C_{11}H_{10}N_3PF_6$: C, 40.12; H, 3.04; N, 12.76. Found: C, 40.07; H, 3.07; N, 12.68.

[(NH$_3$)$_5$Ru−CPI-Me](PF$_6$)$_3$, [1](PF$_6$)$_3$. The mononuclear Ru(II) complex of CPI-Me$^+$ was obtained by reacting 311 mg (1 mmol) of the ligand dissolved in 20 mL of degassed acetone with 512 mg (1 mmol) of [$(NH_3)_5Ru(H_2O)$]$(PF_6)_2\cdot H_2O$[7] in 20 mL of degassed acetone using Schlenk tubes. The reaction is rapid, but the stirring was kept up for 3 h. The final olive-green complex was precipitated using 100 mL of dry degassed diethyl ether. It was filtered off and dried under vacuum. Yield with respect to the metal: 65%.

Anal. Calcd for $C_{11}H_{25}N_8P_3F_{18}Ru$: C, 16.77; H, 4.44; N, 14.23. Found: C, 17.05; H, 4.49; N, 13.81.

IR (KBr, cm^{-1}): 3753 vs br, 3376 s, 2364 vs, 2217 s, 1626 s, 1555 vs, 1510 vs, 1279 s, 1216 vs, 1078 vs, 838 w, 743 s, 560 w.

[(NH$_3$)$_5$Ru−CPI−Ru(NH$_3$)$_5$](PF$_6$)$_4$, [2](PF$_6$)$_4$. The binuclear Ru(II) complex of CPI was obtained by reaction of 84.5 mg (0.5 mmol) of the ligand dissolved in 20 mL of degassed acetone with 512 mg (1 mmol) of [$(NH_3)_5Ru(H_2O)$]$(PF_6)_2\cdot H_2O$ in 20 mL of degassed acetone. Stirring was kept up for 3 h under argon. The final orange-brown complex was precipitated with 100 mL of dry and degassed diethyl ether. It was filtered off as above and dried under vacuum. Yield with respect to the metal: 68%.

Anal. Calcd for $C_{10}H_{37}N_{13}P_4F_{24}Ru_2$: C, 10.70; H, 3.30; N, 16.23. Found: C, 11.05; H, 3.49; N, 15.51.

Table 2. Selected Fractional Atomic Coordinates and Equivalent Isotropic Thermal Parameters (Å^2) for the Non-Hydrogen Atoms of [CPI-Me](PF_6)

atom	*x*/*a*	*y*/*b*	*z*/*c*	*U*(iso)
N(1)	0.2110(3)	−0.5598(5)	−0.2568(4)	0.0643
N(2)	0.3096(3)	−0.0146(4)	−0.2031(3)	0.0399
N(3)	0.3812(3)	0.1332(4)	−0.1732(3)	0.0442
C(1)	0.2462(3)	−0.3505(5)	−0.2374(4)	0.0429
C(2)	0.3183(4)	−0.3169(5)	−0.2392(4)	0.0473
C(3)	0.3397(3)	−0.2068(5)	−0.2277(4)	0.0448
C(4)	0.2880(3)	−0.1302(5)	−0.2144(4)	0.0379
C(5)	0.2163(3)	−0.1617(5)	−0.2120(4)	0.0447
C(6)	0.1949(3)	−0.2727(5)	−0.2238(4)	0.0475
C(7)	0.2253(4)	−0.4670(6)	−0.2493(4)	0.0538
C(8)	0.3828(3)	0.0236(5)	−0.1673(4)	0.0437
C(9)	0.3046(4)	0.1659(5)	−0.2148(4)	0.0509
C(10)	0.2598(4)	0.0754(5)	−0.2331(4)	0.0482
C(11)	0.4502(4)	0.2048(6)	−0.1402(5)	0.0602
N(21)	−0.3646(4)	0.2459(6)	0.4705(5)	0.0828
N(22)	0.0132(3)	0.2650(4)	0.5000(3)	0.0422
N(23)	0.1191(3)	0.2377(4)	0.4711(4)	0.0509
C(21)	−0.2215(3)	0.2568(6)	0.4776(4)	0.0464
C(22)	−0.1803(4)	0.3550(6)	0.4987(5)	0.0561
C(23)	−0.1029(4)	0.3588(5)	0.5056(4)	0.0519
C(24)	−0.0678(3)	0.2625(5)	0.4912(4)	0.0420
C(25)	−0.1082(4)	0.1639(5)	0.4693(4)	0.0495
C(26)	−0.1863(4)	0.1610(5)	0.4620(4)	0.0518
C(27)	−0.3017(4)	0.2520(6)	0.4732(5)	0.0604
C(28)	0.0429(4)	0.2176(5)	0.4413(4)	0.0482
C(29)	0.1393(4)	0.3013(6)	0.5509(5)	0.0553
C(30)	0.0737(4)	0.3197(6)	0.5691(4)	0.0542
C(31)	0.1727(4)	0.2006(7)	0.4246(6)	0.0657
C(41)	0.4671(5)	0.4522(7)	0.1311(5)	0.0947
C(42)	0.3836(4)	0.4690(6)	0.0761(5)	0.0589
C(43)	0.3614(5)	0.4708(8)	−0.0269(5)	0.0828
O(41)	0.3357(3)	0.4779(5)	0.1119(4)	0.0848
P(1)	0.0167(1)	0.0490(1)	0.7448(1)	0.0482
F(1)	0.0221(3)	−0.0815(3)	0.7591(3)	0.0830
F(2)	0.1020(2)	0.0600(4)	0.8236(3)	0.0777
F(3)	−0.0674(2)	0.0349(4)	0.6667(3)	0.0840
F(4)	0.0552(3)	0.0363(4)	0.6671(3)	0.0878
F(5)	0.0114(3)	0.1775(3)	0.7301(3)	0.0875
F(6)	−0.0204(2)	0.0604(4)	0.8242(3)	0.0825
P(10)	0.38553(9)	0.1054(2)	0.0935(1)	0.0513
F(11)	0.4472(9)	0.077(2)	0.043(1)	0.086(6)
F(12)	0.3200(9)	0.046(1)	0.005(1)	0.074(5)
F(13)	0.369(1)	0.221(1)	0.043(1)	0.105(7)
F(14)	0.3316(9)	0.131(2)	0.149(1)	0.096(6)
F(15)	0.4592(9)	0.167(2)	0.175(1)	0.066(5)
F(16)	0.4086(9)	−0.016(1)	0.145(1)	0.074(4)

IR (KBr, cm^{-1}): 3753 vs br, 3435 w, 3305 w, 2363 vs, 2195 s, 1630 s, 1525 s, 1365 vs, 1313 s, 1277 s, 1188 vs, 1104 vs, 1067 vs, 838 w, 744 s, 561 w.

X-ray Crystallography of [CPI-Me$^+$][PF$_6^-$]·0.5acetone. A summary of crystal data is presented in Table 1. The diffraction intensities of an approximately 0.3 × 0.3 × 0.15 mm crystal were collected at room temperature with graphite-monochromatized Mo K_α (0.710 69 Å) radiation using an Enraf-Nonius CAD4 diffractometer. The cell parameters were obtained from the least-squares refinement of the setting angles of 25 reflections with 2θ in the range 26−32°.

A total of 6711 reflections were collected with the $\omega-2\theta$ scan technique to a $2\theta_{max}$ value of 52°. After data reduction, 2880 reflections were considered significant with $I_{net} > 3.0\sigma(I_{net})$. The intensities of two representative reflections measured each hour declined by 29%, probably due to loss of solvent during data collection. A nonlinear smoothed correction factor was applied to the data to account for this phenomenon. The data were corrected for Lorentz and polarization effects but not for absorption.

The structure was solved by direct methods (SIR92[8]). Difference synthesis indicated that the fluorine atoms of one of the anion PF_6^-

(7) Woitellier, S.; Launay, J.-P.; Spangler, C. W. *Inorg. Chem.* **1989**, *28*, 758.

(8) Altomare, A.; Cascarano, G.; Giacovazzo, C.; Guagliardi, A. *J. Appl. Crystallogr.* **1993**, *26*, 343. Altomare, A.; Cascarano, G.; Giacovazzo, C.; Guagliardi, A.; Burla, M. C.; Polidori, G.; Camalli, M., *J. Appl. Crystallogr.* **1994**, *27*, 435.

Table 3. Selected Bond Distances (Å) and Angles (deg) for [CPI-Me](PF_6)

Bond Distances			
N(1)−C(7)	1.142(8)	N(22)−C(28)	1.328(7)
N(2)−C(4)	1.438(7)	N(22)−C(30)	1.387(7)
N(2)−C(8)	1.330(7)	N(23)−C(28)	1.321(7)
N(2)−C(10)	1.381(7)	N(23)−C(29)	1.371(8)
N(3)−C(8)	1.321(7)	N(23)−C(31)	1.468(8)
N(3)−C(9)	1.368(7)	C(21)−C(22)	1.374(9)
N(3)−C(11)	1.458(7)	C(21)−C(26)	1.380(8)
C(1)−C(2)	1.386(8)	C(21)−C(27)	1.441(9)
C(1)−C(6)	1.391(8)	C(22)−C(23)	1.378(8)
C(1)−C(7)	1.446(9)	C(23)−C(24)	1.378(8)
C(2)−C(3)	1.374(8)	C(24)−C(25)	1.372(8)
C(3)−C(4)	1.384(8)	C(25)−C(26)	1.390(8)
C(4)−C(5)	1.374(7)	C(29)−C(30)	1.341(8)
C(5)−C(6)	1.384(8)	C(41)−C(42)	1.46(1)
C(9)−C(10)	1.330(8)	C(42)−C(43)	1.473(9)
N(21)−C(27)	1.137(8)	C(42)−O(41)	1.190(7)
N(22)−C(24)	1.436(7)		
Bond Angles			
C(8)−N(2)−C(4)	125.1(5)	C(30)−N(22)−C(28)	108.1(5)
C(10)−N(2)−C(4)	126.7(5)	C(29)−N(23)−C(28)	108.8(5)
C(10)−N(2)−C(8)	108.0(5)	C(31)−N(23)−C(28)	125.5(6)
C(9)−N(3)−C(8)	108.2(5)	C(31)−N(23)−C(29)	125.7(6)
C(11)−N(3)−C(8)	124.8(6)	C(26)−C(21)−C(22)	120.5(6)
C(11)−N(3)−C(9)	127.0(6)	C(27)−C(21)−C(22)	120.5(6)
C(6)−C(1)−C(2)	120.1(5)	C(27)−C(21)−C(26)	119.0(6)
C(7)−C(1)−C(2)	119.3(6)	C(23)−C(22)−C(21)	120.4(6)
C(7)−C(1)−C(6)	120.6(6)	C(24)−C(23)−C(22)	118.8(6)
C(3)−C(2)−C(1)	120.4(5)	C(23)−C(24)−N(22)	119.3(5)
C(4)−C(3)−C(2)	118.9(5)	C(25)−C(24)−N(22)	119.1(5)
C(3)−C(4)−N(2)	119.3(5)	C(25)−C(24)−C(23)	121.7(5)
C(5)−C(4)−N(2)	119.1(5)	C(26)−C(25)−C(24)	119.1(6)
C(5)−C(4)−C(3)	121.6(5)	C(25)−C(26)−C(21)	119.5(6)
C(6)−C(5)−C(4)	119.4(5)	C(21)−C(27)−N(21)	178.5(8)
C(5)−C(6)−C(1)	119.6(5)	N(23)−C(28)−N(22)	108.8(5)
C(1)−C(7)−N(1)	177.9(7)	C(30)−C(29)−N(23)	107.4(5)
N(3)−C(8)−N(2)	108.8(5)	C(29)−C(30)−N(22)	106.9(5)
C(10)−C(9)−N(3)	108.1(5)	C(43)−C(42)−C(41)	116.3(7)
C(9)−C(10)−N(2)	106.9(5)	O(41)−C(42)−C(41)	122.2(7)
C(28)−N(22)−C(24)	125.6(5)	O(41)−C(42)−C(43)	121.4(7)
C(30)−N(22)−C(24)	126.3(5)		

were disordered. In a first step, refinement of the occupation factors of 12 peaks around the phosphorus atom using slack constraints allowed the localization of three other positions for this PF_6 group. The final relative ratios of these five sites converged to 34.2%, 34.0%, 17.5%, 9.5%, and 5.2% and the occupation factors were then fixed at these values.

Fourier difference synthesis permitted the location of all H atoms in their expected positions. Those of the phenyl and imidazole groups were however positioned geometrically, their location being adjusted after each refinement cycle. The coordinates of methyl H atoms were refined using slack constraints. Final refinements were done with a 6 blocks approximation to the normal matrix using unit weights throughout. A total of 2880 reflections with $I > 3\sigma(I)$ were kept, leading to R values $R = \sum||F_o| - |F_c||/\sum |F_o| = 0.049$ and $R_w = [\sum (|F_o| - |F_c|)^2/\sum|F_o|^2]^{1/2} = 0.0573$. The maximum and minimum residual peaks on the final difference Fourier maps corresponded to +0.36 and −0.26 electron/Å^3 and were found in the vicinity of the disordered PF_6 group. All calculations were performed with the CRYSTALS crystallographic package[9] using an ALLIANT VFX-80 and an IBM RISC6000/580. Drawings were made with ORTEP.[10] Final position parameters of the cations are listed in Table 2, and selected bond lengths and angles are in Table 3.

Spectroscopy and Electrochemistry. UV−vis−near-IR spectra were recorded with a Shimadzu UV-3101 PC spectrophotometer or a Perkin-Elmer Lambda 9 spectrophotometer. IR spectra were recorded in KBr pellets with a Perkin-Elmer 1725 X (FTIR). NMR spectra were recorded with a Bruker WM 250. The proton nomenclature and assignment for some compounds are summarized in Figure 1.

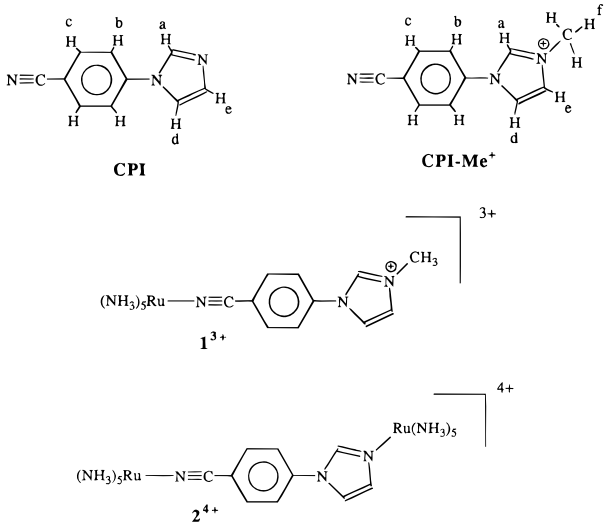

Figure 1. Schematic structures of CPI and CPI-Me$^+$ (with the proton nomenclature for NMR) and of the ruthenium complexes.

Cyclic voltammetry curves were recorded with an Electromat 2000 system from ISMP Technologie (Labège, Haute Garonne, France), using a platinum wire as working electrode, UV grade DMF as solvent, and tetrabutylammonium tetrafluoroborate as supporting electrolyte. The scan rate was 0.1 V s^{-1}, and potentials were measured with respect to the saturated calomel electrode (SCE).

The oxidation of the binuclear complex $\mathbf{2}^{4+}$ has been achieved using two different methods: a chemical one and an electrochemical one. In the first case, well degassed solutions of (TBA)Br_3 10^{-2} M in MeOH and of the complex (10^{-3} M in MeOH) were prepared. A 3 mL aliquot of the complex solution was introduced into a 1 cm cell and titrated by adding aliquots of 30 μL of the oxidizing agent and recording the UV−vis−near IR spectra. Ten additions were necessary for the complete oxidation of both Ru(II) atoms to Ru(III). The electrochemical oxidation was performed by electrolyzing a 3.56×10^{-4} M solution of the complex in DMF at +0.20 V until complete oxidation for 2 h under argon, using a 0.1 M TBATFB solution as supporting electrolyte, a saturated calomel electrode as reference, and a platinum grid as working electrode. At this potential the mixed valence Ru(II)−Ru(III) complex was formed quantitatively. A further electrolysis for 2 h at +0.65 V gave the fully oxidized Ru(III) binuclear complex.

The oxidation of $[(NH_3)_5Ru-CPI-Me]^{3+}$ ($\mathbf{1}^{3+}$) has been achieved using the electrochemical method described previously. For the chemical oxidation, a 10^{-3} M solution of the complex in DMF and a 10^{-2} M solution of (TBA)Br_3 in MeOH were used.

Fluorescence. Uncorrected fuorescence and fluorescence excitation spectra were measured at room temperature with a Jobin Yvon JY3C spectrofluorometer using less than 5×10^{-6} M solutions. Some experiments were also performed with an AMINCO SPF-500C spectrofluorometer interfaced with a HP Vectra microcomputer.

For fluorescence studies, 3-methylpentane (Aldrich 99+%), methylcyclohexane (Aldrich 99+% anhydrous), *n*-butyl chloride (Fluka, for UV spectroscopy), 1-butanol (Merck Uvasol for spectroscopy), ethanol (Carlo Erba absolute, RS for UV spectroscopy), and methanol (Prolabo Spectronorm for UV spectroscopy) were purified by fractional distillation just before measurements.

Computation Techniques. The molecular orbitals and optimized geometry of CPI and CPI-Me$^+$ have been calculated by two different methods: MMX[11] (a molecular mechanics method with quantum treatment of the π part) and MNDO. Both programs were run on an Alliant VFX/80 superminicomputer using the resident parameters of the programs. The effective coupling between metal orbitals through the bridging ligand CPI was computed by the H_{eff} program written by

(9) Watkin, D. J.; Carruthers J. R .; Betteridge, P. W., CRYSTALS, An Advanced Crystallographic Computer Program. Chemical Crystallographic Laboratory, Oxford University.
(10) Johnson, C. K. ORTEP II. Report ORNL-5138; Oak Ridge National Laboratory: Oak Ridge, TN, 1976.
(11) MMX program, version 88.9. Serena Software, Box 3076, Bloomington, IN, 47402−3076.

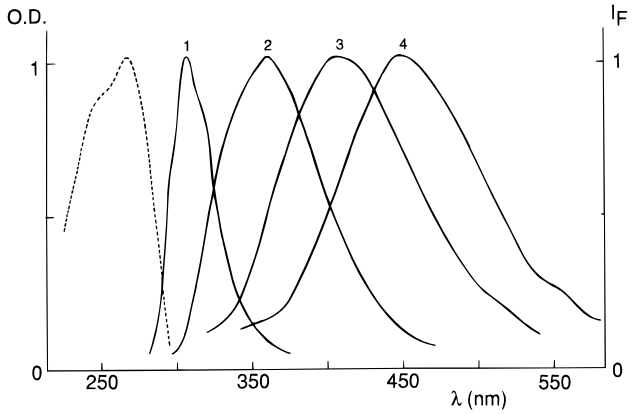

Figure 2. Normalized absorption and fluorescence spectra of CPI in various solvents. Key: dotted curve, absorption spectrum in 3-methylpentane; continuous curves: uncorrected fluorescence spectra in 3-methylpentane (1), *n*-butyl chloride (2), 1-butanol (3), and water (4).

C. Joachim[12] using the output of an extended Hückel calculation. For the latter the ruthenium parameters were taken from Tatsumi and Hoffmann.[13]

Results and Discussion

I. The Ligands. I. 1. General Properties. The reaction of imidazole with 4-fluorobenzonitrile in DMSO gives 1-(4-cyanophenyl)imidazole (CPI) by a standard nucleophilic aromatic substitution. The nature of the final product is proved by NMR and by the crystal structure of CPI-Me^+, showing in particular that the imidazole group is linked by the nitrogen (see below).

UV spectra show the main absorption at 266 nm for CPI (see Figure 2) or 254 mm for CPI-Me^+. By analogy with similar compounds,[3,14,15] this band corresponds to a $\pi-\pi^*$ transition with some character of charge transfer transition (see below).

Cyclic voltammetry of CPI gave no wave in the $-2/+2$ V range. CPI-Me^+ gave one cathodic irreversible wave at -1.625 V due to the reduction of the quaternarized imidazole ring.

I. 2. X-ray Crystal Structure of CPI-Me^+. The crystallographic asymmetric unit contains two CPI-Me^+ cations, two PF_6^- anions and one molecule of acetone. The molecular structures of the cations with the atomic numbering scheme are shown in Figure 3.

Both cation geometries are very close, with the exception of the angle between the benzonitrile mean plane and the imidazolium mean plane (maximum deviation 0.007 Å) which are 31.21(8) and 43.40(8)°. In each cation, the interannular bond is slightly shorter than a single C−N bond [1.438(7) and 1.436(7) Å, to be compared with the N−Me bonds N(3)−C(11) = 1.458(7) and N(23)−C(31) = 1.468(8) Å], indicating a small double bond character.

The two imidazolium groups are very similar and show a nearly perfect C_{2v} symmetry around an axis connecting C(8) or C(28) and the middle of the C(9)−C(10) or C(29)−C(30) bond. As observed in other related compounds,[16−18] the bonding pattern presents two short bonds from C(8) and C(28) [C(8)−N(2) = 1.330(7) Å, C(8)−N(3) = 1.321(7) Å, C(28)−N(22) = 1.328(7) Å, C(28)−N(23) = 1.321(7) Å], one short carbon−carbon bond [C(9)−C(10) = 1.330(8) Å, C(29)−C(30) = 1.341(8) Å] and two longer nitrogen−carbon bond [N(2)−C(10) = 1.381(7) Å, N(3)−C(9) = 1.368(7) Å and N(22)−C(30) = 1.387(7) Å, N(23)−C(29) = 1.371(8) Å]. This pattern seems typical of imidazole groups in which some electron density has been removed. Thus it is observed in 1-methylimidazole complexes with electron deficient metals.[18] In the present case, it is the methylation which drains some electron density and thus plays the same role as complexation.

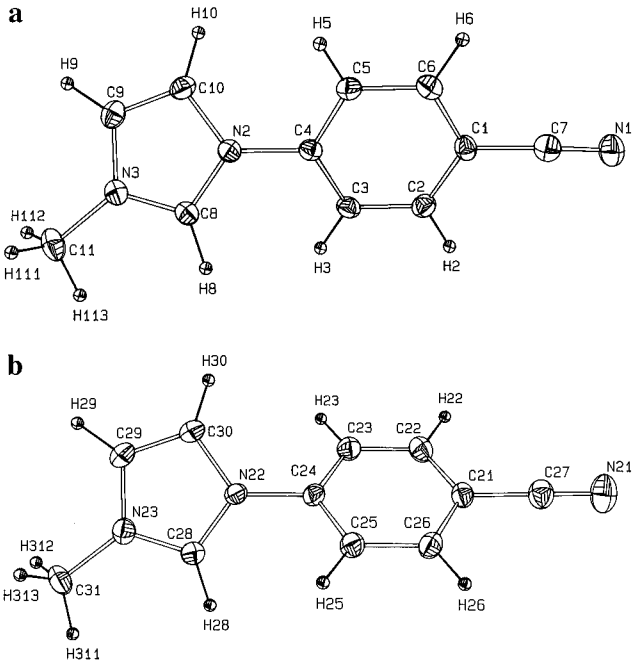

Figure 3. Structure of CPI-Me^+. The two independent molecules of the asymmetric unit are shown with the atom numbering.

Finally, in the crystal, the benzonitrile groups of the two cations pack in nearly parallel planes with an angle between the planes C(1) to C(6) and C(21) to C(26) of 8.63(7)°, whereas the imidazoyl groups are at 62.55(9)°.

I. 3. Theoretical Calculations. Theoretical calculations have been undertaken mainly to obtain more information about the ligand geometry in its ground state. Although crystals of CPI have been obtained, the resolution of the crystal structure failed. Thus the only structural result available concerns CPI-Me^+ which is found twisted, as mentioned above. However, this does not prove that CPI itself is twisted, because a strong electronic rearrangement is associated with quaternarization of the imidazole nitrogen, so that CPI-Me^+ cannot be considered as made of a donor and an acceptor part. In addition, the exact geometry of the isolated molecule could be slightly different from the one observed in the crystal, due to the occurence of crystal packing forces.

We have thus performed theoretical calculations using two different semiempirical methods : MMX (a molecular mechanics program taking into account π interactions by a variable electronegativity SCF procedure[19]) and MNDO. Both methods have been used to predict the ground state geometry and determine the composition of the π molecular orbitals (i.e. the coefficients of the LCAO expansion). MNDO is known to give a good correlation with *ab initio* calculations,[20] in particular for electrostatic charges. Concerning molecular mechanics, MMX was chosen because of its good force field incorporating

(12) Joachim, C. H_{eff} program. CEMES, Toulouse.
(13) Tatsumi, K.; Hoffmann, R. *J. Am. Chem. Soc.* **1981**, *103*, 3328.
(14) Rettig, W.; Marschner, F. *Nouv. J. Chim.* **1983**, *7*, 425.
(15) Rettig, W. *J. Mol. Struct.* **1982**, *84*, 303.
(16) Kratochvil, B.; Ondracek, J.; Velisek, J.; Hasek, J. *Acta Crystallogr.*, C **1988**, *44*, 1579.
(17) Alcade, E.; Dinarés, I.; Frigola, J.; Jaime, C.; Fayet, J.-P.; Vertut, M.-C.; Miravitlles, C.; Rius, J. *J. Org. Chem.* **1991**, *56*, 4223.
(18) Johnson, C. R.; Jones, C. M.; Asher, S. A.; Abola, J. E. *Inorg. Chem.* **1991,** *30*, 2120 and references therein.
(19) Brown, R. D.; Hefferman, M. L. *Aust. J. Chem.* **1959**, *12*, 319.
(20) Aleman, C.; Luque, F. J.; Orozco, M. *J. Comput. Chem.* **1993**, *14*, 799.

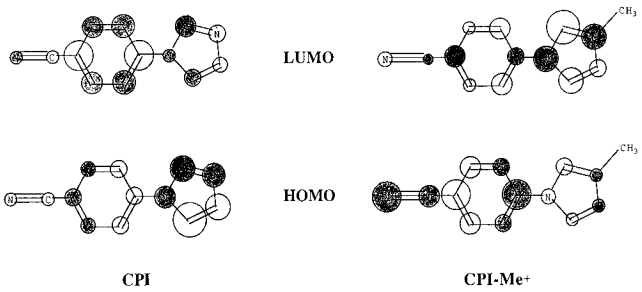

Figure 4. Shape of the frontier orbitals in CPI and CPI-Me$^+$ from MMX calculations. For CPI-Me$^+$, the calculation has been performed with a 33° twist angle and the drawing is made in the mean plane of the molecule.

a variable electronegativity SCF calculation for the π part, and also for its potentiality to treat, in a future study, open shell systems.

For CPI, MMX predicts a planar geometry in the ground state. The study of the energy as a function of the dihedral angle between the benzonitrile and the imidazole ring shows the 90° twisted form to be less stable by *ca*. 5 kcal. The HOMO of this planar form appears to be located mainly on the imidazole part (see Figure 4). The LUMO is mostly located on the phenyl ring (see Figure 4). Thus the first electronic transition has indeed a charge transfer character from the imidazole part toward the benzonitrile part. Finally the bond order between atoms connecting the imidazole and the benzonitrile is 1.27, indicating a rather strong interaction between the two parts of the molecule.

MNDO calculations lead to similar conclusions. The molecule is also found planar, and the frontier orbitals are very similar. The bond order is slightly less (1.10) than found by the MMX method.

In the case of CPI-Me$^+$, MMX and MNDO predict a non planar geometry with a 33.3 (MMX) or 23.4° (MNDO) dihedral angle (in the two cases, all geometrical parameters were free for a complete optimization). This is to be compared with the values obtained by crystallography: 31° for one of the independent molecules of the asymmetrical unit and 43° for the other. The fact that two markedly different values are obtained in the crystal structure shows that the molecule is certainly not very rigid, in agreement with the low C4−N2 bond order (see below). Thus the results of the calculations can be considered as satisfactory.

For the frontier orbitals of CPI-Me$^+$, both methods give a HOMO located on the benzonitrile moiety, while the LUMO is mainly localized on the imidazolium ring (see Figure 4). Thus there is a reversal with respect to the case of CPI; i.e. *the imidazole part is no longer a donor group*. This is obviously due to the quaternarization of the external nitrogen. A confirmation is provided by the NMR shifts. Thus the proton chemical shifts for CPI are close to those observed for betaines of the azolium azolate type[21] in which there is some charge transfer from the negative part toward the imidazolium part of the molecule. So in the present case, we can also assume that there is a partial charge transfer reducing the effective charge on the imidazole ring.

The bond order between C4 and N2 (see Figure 3a for nomenclature) was computed as 1.07 (MMX) or 0.97 (MNDO) *for an imposed planar geometry* (for the twisted geometry, the figures were 1.04 and 0.96 respectively). Thus, for the same planar geometry, the π interaction between the two parts of the molecule has been greatly reduced with respect to CPI. This is probably the reason why the molecule is no longer planar.

(21) Alcade, E.; Dinarés, I. *J. Org. Chem.* **1991**, *56*, 4233.

Table 4. Maximum Wavelengths for Absorption, Fluorescence,[a] and Fluorescence Excitation[a] of CPI at Room Temperature as a Function of Solvent Polarity

		λ_{max} (nm)		
solvent	dielectric constant	absorption	fluorescence	fluorescence excitation
3-methylpentane	1.9	267	306	277
methylcyclohexane	2.0	267	308	277
n-butylchloride	7.4	266	359	275
1-butanol	17.5	263	405	273
ethanol	24.3	262	415	272
methanol	32.6	261	427	271
water	78.5	257	445	270

[a] From uncorrected spectra.

To summarize, for the case of CPI-Me$^+$ where the crystal structure is available, there is a satisfactory agreement between the results of these theoretical methods and the experiment. Consequently, we can state with a large degree of confidence that CPI is planar in the ground state. This is confirmed by *ab initio* calculations.[22]

I. 4. Absorption and Luminescence Properties. The absorption and the corresponding fluorescence maxima of CPI in solvents of different polarity are presented in Table 4 and Figure 2. The maxima of the uncorrected fluorescence excitation spectra are also given in this table. Whatever the solvent polarity and the emission wavelength, the excitation spectra present a unique band similar to the corresponding absorption spectra (Table 4). In nonpolar solvents, such as 3-methylpentane, a fluorescence band with a maximum at 306 nm is observed. This band is strongly shifted to the red when the solvent polarity increases (Table 4). The solvatochromic red shift of about 10 200 cm^{-1} between 3-methylpentane (λ_{max} = 306 nm) and water (λ_{max} = 445 nm), is accompanied by a broadening of the fluorescence band (see Figure 2). It is higher than that observed for DMABN but is similar to that observed for N-pyrrolyl-4-benzonitrile (PBN)[14] whose electronic structure is closely related to that of CPI. For PBN, as for DMABN, the fluorescence band is assigned to a TICT state.[14,15] Thus by analogy with PBN, we attribute also the fluorescence of CPI to a TICT state.

II. Ruthenium Complexes. II. 1. CPI as Bridging Ligand. The interaction of CPI with $[Ru(NH_3)_5(H_2O)]^{2+}$ in acetone yields the binuclear complex in which one ruthenium is linked to the nitrile end and the other to the imidazole ring. In the case of CPI-Me$^+$, a monometallic complex is obtained, since there is only one coordination site, the nitrile end.

II. 2. Electrochemical and Spectroscopic Properties of $[(NH_3)_5Ru-CPI-Me]^{3+}$ ($\mathbf{1}^{3+}$) and $[(NH_3)_5Ru-CPI-Ru(NH_3)_5]^{4+}$ ($\mathbf{2}^{4+}$). Electrochemical and spectroscopic properties of $\mathbf{1}^{3+}$ and $\mathbf{2}^{4+}$ are summarized in Table 5. The comparison between the two complexes greatly helps the assignment of oxidation waves and absorption bands because in $\mathbf{1}^{3+}$, the only available coordination site is the nitrile end.

For $\mathbf{1}^{3+}$, UV−vis spectra in methanol (see Figure 5) show a first band at 252 nm (ϵ = 15 400), which is due to an intraligand $\pi-\pi^*$ transition, and a second at 420 nm (ϵ = 3000), which is assigned to a metal-to-ligand charge transfer band of the pentaammineruthenium−benzonitrile moiety (cf. the observed λ_{max} for analogous pentaammineruthenium complexes of the following: benzonitrile, 376 nm;[23] dmabn, 342 nm;[24,25] bcppz, 365 nm[6]). The location of this charge transfer band depends

(22) Lepetit, M.-B.; Hatzidimitriou, A. Unpublished results.
(23) Clarke, R. E.; Ford, P. C. *Inorg. Chem.* **1970**, *9*, 227.
(24) Sowinska, M.; Launay, J.-P.; Mugnier, J.; Pouget, J.; Valeur, B. *J. Photochem. Photobiol. A: Chem.* **1987**, *37*, 69.

Table 5. Spectral and Electrochemical Data for $\mathbf{1}^{3+}$ and $\mathbf{2}^{4+}$

compound	λ_{max}, nm (ϵ, M^{-1} cm^{-1})[a]	E_p,[b] V	
		cathodic	anodic
$\mathbf{1}^{3+}$	252 (15 400), 420 (3 000)	−1.65 (irr)	+0.38 (rev)
$\mathbf{2}^{4+}$	258 (20 700), 415 (10 100)		−0.05 (rev), +0.37 (rev)

[a] In methanol. [b] Peak potentials in DMF vs SCE. rev = reversible peak; irr = irreversible peak.

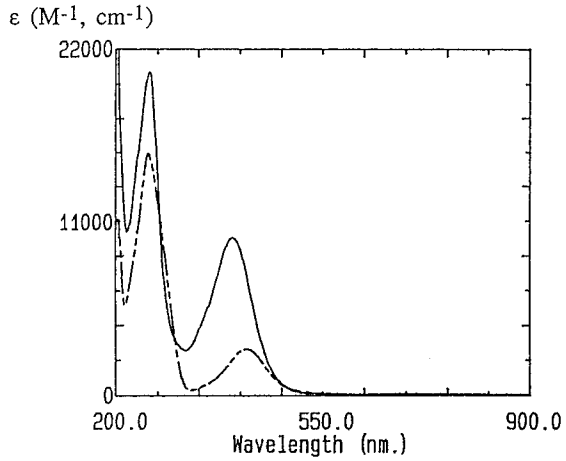

Figure 5. UV-visible spectra of $\mathbf{1}^{3+}$ (− --) and $\mathbf{2}^{4+}$ (—) in methanol.

in a sensitive way upon the substituent on the benzonitrile ligand: thus with respect to the benzonitrile complex, the band has moved toward longer wavelengths (lower energies), which can be assigned to the acceptor properties of the imidazolium moiety. Incidentally, this shows that the imidazolium and ruthenium group communicate through the benzonitrile part.

Cyclic voltametry of $\mathbf{1}^{3+}$ gives two waves: The first is a reversible anodic wave at + 0.380 V corresponding to the pentaammineruthenium(II/III) couple linked to nitrile. The second, which is cathodic and irreversible is found at −1.650 V and is assigned to the reduction of the quaternarized imidazole ring.

For $\mathbf{2}^{4+}$, UV−vis spectra in methanol gave two bands, at 258 nm (ϵ = 20 700) and at 415 nm (ϵ = 10 100), as shown in Figure 5. As for $\mathbf{1}^{3+}$, we assign the first band to the intraligand $\pi-\pi^*$ transition, and the second one to the metal-to-ligand charge transfer band of the pentaammineruthenium−benzonitrile moiety. In addition, one could expect a metal-to-ligand charge transfer involving the imidazole part of the molecule. The comparison with $[(NH_3)_5Ru-imidazole]^{2+}$ [26,27] suggests that it occurs in the same range as the ligand $\pi-\pi^*$ band.

Cyclic voltammetry of $\mathbf{2}^{4+}$ gave two well-separated reversible anodic waves close to −0.050 V and +0.370 V (Figure 6). Using $\mathbf{1}^{3+}$ data, the first is assigned to imidazole-bound ruthenium, and the second to nitrile-bound ruthenium. These values are in agreement with the known redox potentials of ruthenium pentaammine groups N-linked to imidazole[27,28] or to substituted benzonitrile compounds.[6,24]

When the benzonitrile and imidazole ligands are compared, it is clear that benzonitrile is a rather good acceptor, while imidazole is a poor acceptor and probably in fact a π donor. Thus, the former shifts the redox potential toward positive values and gives the lowest energy charge transfer transition, as a result of the more efficient π back-bonding with ruthenium(II).

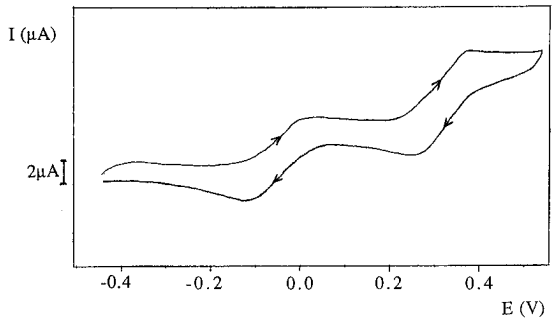

Figure 6. Cyclic voltammetry of $\mathbf{2}^{4+}$ in DMF.

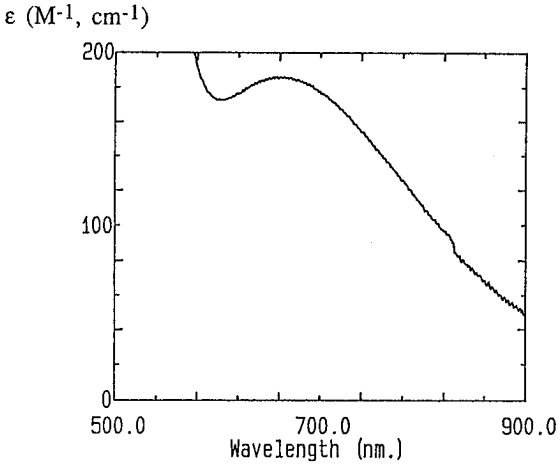

Figure 7. Intervalence transition for $\mathbf{2}^{5+}$ in methanol.

The difference in oxidation potentials confers to the present system a distinct advantage over complexes with symmetrical ligands, because it allows the quantitative preparation of the mixed valence species.

II. 3. Intervalence Transition and Metal−Metal Coupling through CPI. During the chemical oxidation of $\mathbf{2}^{4+}$ in MeOH, a decrease of the MLCT band of the fragment Ru−nitrile at 392 nm was observed. This band disappeared completely only after the addition of 1 mol of $(TBA)Br_3$ per mole of complex, corresponding to the complete oxidation of the binuclear complex. A new band appears, at 320 nm which is assigned to a ligand-to-metal charge transfer band of the Ru(III)−imidazole moiety. A weak band appears at 640 nm and reaches a maximum intensity at half-oxidation, after which it decreases (maximum ϵ = 188 for the spectra of the sixth addition). It is assigned to the intervalence transition due to the Ru(II)−Ru(III) pair linked by CPI (see Figure 7). In this mixed-valence compound, the ruthenium coordinated to the cyanophenyl group is ruthenium(II) while the ruthenium linked to imidazole is ruthenium(III).

The spectra at half-oxidation and full oxidation are identical with the ones observed in the electrolysis successively at + 0.2 and + 0.65 V in the same medium. The electrochemical oxidation was found to be reversible; i.e., the starting compound could be regenerated by reduction.

Finally, oxidation experiments (chemical and electrochemical) were also performed in DMSO. In this case, the intervalence transition was observed at 660 nm.

(25) Curtis, J. C.; Sullivan, B. P.; Meyer, T. J. *Inorg. Chem.* **1983**, *22*, 224.
(26) Shepherd, R. E.; Taube, H. *Inorg. Chem.* **1973**, *12*, 1392.
(27) Sundberg, R. J.; Bryan, R. F.; Taylor, I. F.; Taube, H. *J. Am. Chem. Soc.* **1974**, *96* , 381.
(28) Tweedle, M. F.; Taube, H. *Inorg. Chem.* **1982**, *21*, 3361.

The chemical oxidation of the Ru−CPI-Me$^+$ ($\mathbf{1}^{3+}$) complex has been achieved with the same procedure described for the Ru−CPI-Ru complex. In this case there is no intervalence band, as expected, only a decrease of the optical density in the MLCT band range of the fragment Ru−nitrile near 412 nm.

Since the two oxidation waves of $\mathbf{2}^{4+}$ are widely separated, the formation of the mixed valence species $\mathbf{2}^{5+}$, i.e. Ru(III)−CPI−Ru(II) is almost quantitative. From the difference in redox potentials a value of 1.25×10^7 is computed for the comproportionation constant. This high value is compatible with the shape of the optical density versus oxidant equivalent plot in the chemical titration. Thus at half-oxidation, or after electrolysis at + 0.20 V, the proportion of mixed-valence species is computed to be near 100%.

The analysis of the intervalence band provides some insight on the degree of metal−metal coupling. The intervalence band is rather clearly resolved; however we have performed a spectral deconvolution using a technique already described[29] to extract more accurate parameters. In methanol, the results were as follows: a band position $\bar{\nu}_{max} = 15\,380$ cm^{-1}, a full width at half-maximum $\Delta\bar{\nu}_{1/2} = 9030$ cm^{-1} and a true extinction coefficient $\epsilon = 185$ M^{-1} cm^{-1}. Introducing these values into the Hush equation[30] gives the metal−metal coupling through the bridging ligand $V_{ab} = 262$ cm^{-1} (0.032 eV). This value is comparable to the one observed in several conjugated systems, for example ruthenium pentaammine groups linked by bipyridyl heterocycles[29] or ruthenium terpyridyl groups linked by bis(terpyridyl)[31] or bis(cyclometalating)[32] ligands.

Thus contrary to the case of BCPPZ, there is an appreciable coupling in the present case. This is clearly due to the conjugated character of the CPI ligand with its planar structure.[33] This was confirmed by a theoretical estimation of the metal−metal coupling using the effective Hamiltonian theory.[34] We have first performed an extended Hückel molecular orbital calculation on $[(NH_3)_5Ru-CPI-Ru(NH_3)_5]^{4+}$ after geometry optimization by MMX of the free ligand. From the output (eigen values and vectors) the effective matrix element between the two d orbitals of the ruthenium atoms exhibiting π symmetry (i.e. able to mix with the ligand π system) was computed using the Heff program.[12] This gave $V_{ab} = 0.028$ eV, in satisfactory agreement with the experimental value.

II. 4. Photochemical Properties of $[(NH_3)_5Ru-CPI-Ru(NH_3)_5]^{4+}$ ($\mathbf{2}^{4+}$). The binuclear complex $\mathbf{2}^{4+}$ was found to be weakly emitting when excited either in the 250−260 nm range or in the 400−420 nm range. Solubility and photostability considerations limited the study to ethanol, methanol, and water.

The 250−260 nm range corresponds essentially to the ligand-based absorption. In ethanol, the emission is the most intense but occurs at the same position as for the free ligand. In methanol and water, a weak emission with a structured spectrum is obtained (Figure 8). Again, one of the peaks occurs at the same wavelength as for the free ligand, but the general shape of the spectrum is markedly different, and a new emission clearly distinct from the one of the free ligand is obtained at 310 nm in methanol and water. Although the spectra have been recorded on freshly prepared solutions, these results suggest that some decomplexation could occur upon irradiation, due to the short wavelength of the excitation. Thus the complex emits undoubtedly at 310 nm but could also contribute to the higher wavelengths emission. Since the solvent effect is very small and solubility considerations preclude the use of other solvents, this study gives no evidence for a TICT effect in the coordinated ligand when excited on the $\pi-\pi^*$ transition.

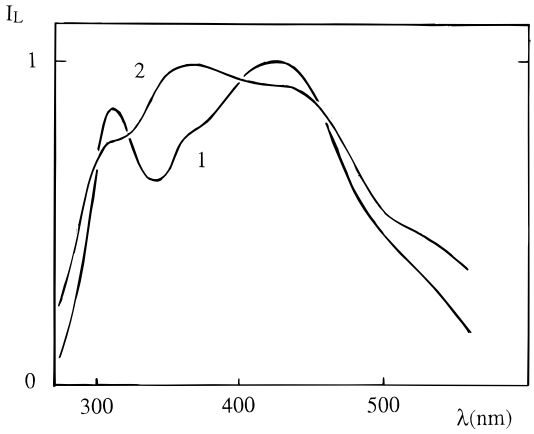

Figure 8. Normalized luminescence spectra of $\mathbf{2}^{4+}$ in methanol (1) and water (2) observed when exciting at 258 nm.

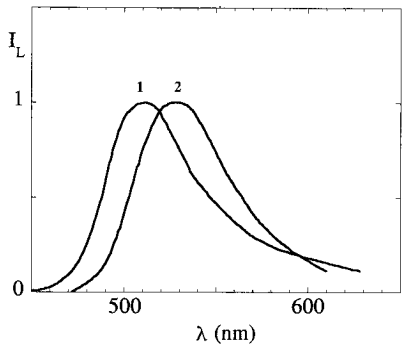

Figure 9. Normalized luminescence spectra of $\mathbf{2}^{4+}$ in ethanol (1) and water (2) observed when exciting at 410 nm.

When excitation is performed in the 400−420 nm range, corresponding to the metal-to-benzonitrile charge transfer, the emission is very weak but cannot be attributed to the free ligand, because it does not absorb in this range. Moreover, the emission spectrum is not structured and the excitation spectrum parallels the absorption spectrum. Thus, there is no interference due to photoinduced decomplexation, probably as a result of the lower photon energy. The emission is observed at 510 nm in ethanol and 528 nm in water (Figure 9). This noticeable solvent effect implies some polarity for the excited state, which is not unexpected because it has a charge transfer (metal-to-ligand) character. Due to the impossibility to realize a thorough study in a wide range of solvents, no clear conclusion can be drawn about the geometries of the ground and excited states. It is only possible to speculate that since the LUMO of the ligand is antibonding between the imidazole and benzonitrile parts (see Figure 4), its population should reduce the bond order and favor some twisting in the excited state.

(29) Ribou, A.-C.; Launay, J. P.; Takahashi, K.; Nihira, T.; Tarutani, S.; Spangler, C. W. *Inorg. Chem.* **1994**, *33*, 1325.
(30) Hush, N. S. *Coord. Chem. Rev.* **1985**, *64*, 135.
(31) Collin, J.-P.; Lainé, P.; Launay, J.-P.; Sauvage, J.-P.; Sour, A. *J. Chem. Soc., Chem. Commun.* **1993**, 434.
(32) Beley, M.; Chodorowski-Kimmes, S.; Collin, J.-P.; Lainé, P.; Launay, J.-P.; Sauvage, J.-P. *Angew. Chem., Int. Ed. Engl.* **1994**, *33*, 1775.
(33) Strictly speaking, there is no proof that for the ruthenium complexes in their different oxidation states, the CPI ligand is still planar. However the orbital overlaps are not drastically affected by a moderate twist, so that the theoretical conclusions remain qualitatively valid. In any case, the noticeable experimental V_{ab} coupling excludes a severely twisted structure in the mixed valence state.
(34) Joachim, C.; Launay, J.-P. *Chem. Phys.* **1986**, *109*, 93. Woitellier, S.; Launay, J.-P.; Joachim, C. *Chem. Phys.* **1989**, *131*, 481. Joachim, C.; Launay, J.-P.; Woitellier, S. *Chem. Phys.* **1990**, *147*, 131.

Conclusion

The cyanophenylimidazole ligand is predicted to be planar according to theoretical studies and presents interesting emission properties suggesting the existence of a TICT state. Moreover it can be used as bridging ligand to prepare a mixed valence complex in which ruthenium(III) is linked to imidazole while ruthenium(II) is linked to the nitrile end. The intervalence transition shows a moderate coupling (0.032 eV) between the metal sites, suggesting that the ligand remains planar or near planarity upon complexation. The ligand luminescence is strongly quenched in the ruthenium complexes but does not disappear completely, and there is some emission coming from a metal-to-ligand charge transfer excited state. Although the present work provides no definitive proof for the existence of a TICT effect in the complex, this type of ligand offers interesting perspectives for the study of intramolecular metal-to-metal (intervalence) charge transfer as well as photoinduced geometrical changes.

Acknowledgment. Thanks are due to Malgorzata Sowinska ("Goska"), from Wroclaw Technical University, for the initial discovery of CPI during her post-doctoral stay at Université Pierre et Marie Curie, Paris, 1986. We are also indebted to Ministère de la Recherche et de la Technologie for a post-doctoral fellowship to A.H. and also to the EC program "Human Capital and Mobility" for fellowships to E.M. and A.H. Finally we thank Mrs A. Barat (Université Paris Sud) for experimental help and A. Lopez (Institut de Biologie Cellulaire et Génétique, Toulouse) for fluorometer facilities.

Supporting Information Available: For the crystal structure, listings of crystal and refinement data, fractional atomic coordinates including H and PF_6, anisotropic temperature factors, and bond distances and angles (12 pages). Ordering information is given on any current masthead page.

IC950493M